

**SHORT THESIS FOR THE DEGREE OF DOCTOR OF
PHILOSOPHY (PHD)**

**Investigation of the role of cytoskeletal protein
Septin7 in C2C12 cell cultures**

Zsolt Ráduly Pharm.D.

Supervisor: Dr. Mónika Szentandrásyné Gönczi



UNIVERSITY OF DEBRECEN
DOCTORAL SCHOOL OF MOLECULAR MEDICINE

DEBRECEN, 2023

Investigation of the role of cytoskeletal protein Septin7 in C2C12 cell cultures

By Zsolt Ráduly, Pharmacist

Supervisor: Dr. Mónika Szentandrásyné Gönczi

Doctoral School of Molecular Medicine, University of Debrecen

Head of the **Defense Committee**: László Virág, PhD, DSc

Reviewers: Endre Károly Kristóf, PhD
Anikó Keller-Pintér, PhD

Members of the Defense Committee: Bernadett Éva Trencsényiné Balázs, PhD
Máté Ágoston Demény, PhD

The PhD Defense takes place at Department of Internal Medicine, building "A" classroom,
Faculty of Medicine, University of Debrecen, 31st January, 2024, 14.00

1. Introduction

Rapid recovery from musculoskeletal injuries has a major health, social and economic role. When most new medicines are authorized, side effects on skeletal muscle must always be included in the reaction profile, as they carry a serious pharmacovigilance risk. Any new information on the skeletal muscle could be a potential therapeutic direction to improve people's lives. The cytoskeletal system was already described and characterized by the end of the 20th century, so the role of actin, intermediate filaments or microtubules is relatively well known. However, research over the last 50 years has highlighted the fact that another major protein group, the septins, also play a prominent role in the structure and regulation of the cytoskeleton. Our research has explored a hitherto unknown area where we examined the role of septins, and more specifically Septin7, in skeletal muscle. Our group described for the first time their role in skeletal muscle *in vitro* and *in vivo*, which provides a new direction for science in understanding the processes of skeletal muscle development and regeneration. In this thesis we present the results from *in vitro* experiments carried out on C2C12 cells.

2. Literature overview

2.1 *The skeletal muscle and myogenesis*

The skeletal muscle is made up of bundles of muscle fibers surrounded by a layer of connective tissue. Skeletal muscle fibers vary in size, ranging from 10 to 80 μm in diameter and from a few mm to 25 cm in length. The striated multinucleated muscle fibers form the cellular and functional units of skeletal muscle. The formation of muscle fibers during prenatal ontogenesis is the result of a tightly programmed series of events regulated by a multitude of signal transduction processes, a process known as myogenesis.

Myoblasts are embryonic precursors of myocytes (also known as muscle cells). During myogenesis, myoblasts fuse (fusion) into multinucleated myotubules, which later develop into muscle fibers after appropriate innervation.

The development of skeletal muscle is not limited to the prenatal period, as this organ has a high regenerative capacity. In the process, the existing system is repaired by a dormant satellite cell (SC) population, whose main role is to regenerate muscle tissue and maintain dormant SCs. To achieve this, SCs can divide symmetrically and asymmetrically. During an asymmetric process, a single SC can generate a self-renewing daughter cell, retaining its Pax7 expression and repressing MyoD (Pax7^{high}/MyoD^{low}), and a committed cell in which it represses Pax7 and

expresses MyoD ($\text{Pax7}^{\text{low}}/\text{MyoD}^{\text{high}}$). If the delicate balance between self-renewal and commitment is upset, this can lead to a failure of the regeneration process and/or depletion of the stem cell reserve. In addition to fusion and differentiation, it is very important for committed SCs to reach the right place, which is achieved by cell migration.

2.2 *Structure of the skeletal muscle cytoskeletal system and its role in migration*

During skeletal muscle development and regeneration, the rearrangement of cytoskeletal elements and the regulation of cell adhesion processes are the main drivers of migration processes. The cytoskeleton is a complex system composed from microtubules, intermediate filaments and microfilaments. Research findings over the last 50 years suggests that another major protein family, the septins, constitute the fourth element of the cytoskeletal system. Many regulatory factors are involved in the migration of myoblasts, but most of these are not muscle specific. The process is significantly influenced by the dynamic rearrangement of the cytoskeleton. The main protein involved is actin, which is organized into complex structures (filopodia, lamellipodia, stress fibers or podosomes). Within stress fibers, the contractile properties of the actomyosin complex are regulated by proteins located in the adhesion complexes of the plasma membrane. Examples include small GTPases of the Rho family (Rho1, Cdc42 and Rac1), which target other complexes, including Arp2/3, in the regulation of subcellular actin assembly, the latter also having a role in the regulation of filament branching. In addition, several studies have shown that the above-mentioned proteins interact not only with actin filaments but also with other cytoskeletal proteins, such as the septins, which molecules are in the focus of the present thesis.

2.3 *Septins*

2.3.1 Septins in general

Septins are guanosine triphosphate (GTP)-binding proteins and belong to a highly conserved family of proteins in eukaryotes. Important roles for septins have been demonstrated in a variety of physiological and pathological cellular processes, including carcinogenesis, exocytosis, endocytosis, and cell division. To date, 13 human septin proteins have been identified and classified into four groups based on sequence similarity (SEPT2, SEPT3, SEPT6, SEPT7). Septins are proteins with highly diverse structures that can react with each other to form even

more complex structures. To function as higher-order protein structures, the presence of representatives of specific septin groups (SEPT2,3,6,7) in the complexes is very important. The resulting complex may be able to react with other proteins at several points simultaneously. The organization of septin filaments involves the binding and hydrolysis of nucleotides.

The structure of the septins includes a GTP-specific motif (AKAD) and Walker A (GxxxxGKS/T) and B (DxxG) motifs, which interact with the guanine subunit of GTP and also facilitate GTP hydrolysis by binding to the phosphate groups of GTP and involving an Mg^{2+} . In contrast to the monomeric small GTPases of the Ras superfamily, the septins oligomerize through their GTP-binding domains (G interface), forming filamentous hetero-polymers. Several domains play a prominent role in the structure of septins. The NC interface represents the N-terminal and C-terminal parts of the protein. These include the Septin Unique Element (SUE), which extends from the G to the NC surface and allows filament formation, the Coiled Coil motif, which together with other polybasic domains (PB1 and PB2) in septins can facilitate membrane interaction, and the N-terminal domain, which is usually disordered in structure and also promotes membrane interaction.

According to the crystal structure of the oligomers studied, the NC interface is the interaction points between the subunits, and interaction can also be achieved using the surface of the G-interface. The mapping of septin complexes and their interacting protein partners is an area of intense scientific research today. As the only member of SEPT7 group, and based on the group assignment and structural knowledge, Septin7 plays an essential role in the formation of hetero-oligomeric septin complexes and thus higher order cytoskeletal structures.

2.3.2 Description of the Septin7 protein

The gene sequence encoding Septin7 (*SEPTIN7*) contains 1254 nucleotides on chromosome 7P14.4-14.1, encoding 418 amino acids, including the GTP-binding motif. The cDNA sequence of Septin7 in humans is homologous to *cdc10* in yeast, initially *Septin7* in humans was called *hCdc10*. Based on the three-dimensional X-ray structure of each septin, it has been shown that Septin7, like other septins, contains a canonical Ras-like G-domain consisting of 6 β -strands and 5 α -helices. Septin7 forms a dimer through a G-interface. The role of Septin7 has been described in many cellular processes. Several studies have demonstrated its role in various tumor lesions, such as certain gliomas, papillary thyroid carcinoma (PTC) and hepatocellular carcinoma, but there are also data on its role in intracellular calcium homeostasis. It is important to note that the role of different septins often appears to be controversial in different

experimental systems. For example, the expression of Septin7 in different glioma cell lines was lower than in normal brain cells, therefore elevated expression of Septin7 significantly inhibited LN18 cell migration and IGF-1-induced chemotaxis. It was also shown that increased Septin7 expression could depolymerize actin filaments, thus inhibiting glioma cell migration. In contrast, reduced expression of Septin2 and Septin7 resulted in inhibited proliferation, migration and invasion on breast cancer cell lines. In human osteosarcoma U2-OS cells, Septin7 was able to maintain cell migration by modulating microtubule nucleation, whereas lower Septin7 expression decreased migration of these cells.

2.3.3 Options for modifying the organization of the septin system

There are several ways to study migration processes, but it is essential to develop and understand compounds that act through the regulation of septins. Forchlorfenuron (FCF; N-(2-chloro-4-pyridyl)-N9-phenylurea; CPPU) is a small molecule compound known to reversibly affect the assembly of septin filaments. According to the measurements of *Angelis et al*, docking of FCF with all known crystal structures of septins indicates that FCF favours the GTP-binding pocket. They found that the binding free energies and affinity of FCF can vary *in silico* depending on the septin groups, suggesting that FCF may access or fit some nucleotide pockets of certain septins better than others, thereby affecting hydrolysis.

3 Aims and Objectives

The role of the septins in skeletal muscle has not been comprehensively studied in the last 50 years, which has prompted us to explore the current gaps in knowledge in this field. Our group planned to investigate the role of septins using *in vitro* and *in vivo* models. In this thesis the *in vitro* results obtained on C2C12 cells are presented. C2C12 is an immortalized mouse-derived myoblast cell line, which is an accepted model system for studying mammalian skeletal muscle development.

In our research we have set up the following objectives:

- Analysis of septin expression on myoblasts and at different stages of myotube differentiation.
- Studying the role of Septin7 in C2C12 cells; modifying the expression of the protein by CRISPR/Cas9-induced gene knockout and shRNA-based gene silencing and determining the cellular parameters of the resulting cell cultures.

- To clarify the role of the Septin7 protein in C2C12 cell migration.
- - Exploring the role of Septin7 in intracellular Ca²⁺ homeostasis related to cell migration in C2C12 cultures.
- Description of the effects of pharmacological inhibition of septins on C2C12 cell migration.

4 Materials and Methods

4.1 C2C12 cell culture and differentiation

The mouse-derived C2C12 myoblasts (ATCC, Cat# CRL-1772; RRID: CVCL_0188) were cultured in high glucose nutrient solution (Dulbecco's Modified Eagle Medium (DMEM, Biosera, Nuaille, France) containing 10 vol/vol% (V/V%) fetal bovine serum (FBS, (Gibco Life Technologies, Carlsbad, CA, USA), antibiotics Penicillin (100 IU/mL) and Streptomycin (100µg/mL) (Biosera), and L-glutamine (Biosera) at 2mM concentration. The culture medium was changed every other day and cell passaging was performed after reaching 80-90% confluency.

In experiments, when C2C12 cells reached 80-90% confluence, cells were washed with PBS and then cultured in differentiation media. The differentiation media was DMEM based, containing 2 V/V% horse serum (Horse Serum, HS, Gibco, Billings, Montana, USA), antibiotics penicillin (100 IU/mL) and streptomycin (100 µg/mL) (Biosera), and L-glutamine (Biosera) at 2mM concentration. The prepared media was used during the differentiation process (myotube formation).

4.2 Proliferation assays

Cell proliferation was assessed using the CyQUANT NF Cell Proliferation Assay Kit (Invitrogen, Carlsbad, California, USA). C2C12 cells (2500 cells/well) were cultured in a 96-well black cell culture dish (Greiner Bi-One, Mosonmagyaróvár, Hungary) for 72 h. On the day of measurement, we followed the manufacturer's instructions. In brief, 1x HBSS (Hank's balanced salt solution) buffer was prepared with deionized water using the provided 5x HBSS, and then CyQUANT NF dye reagent (preparation of 1x dye binding solution) was added. Before the measurement, the proliferation media was replaced with 100 µl of 1x dye binding solution, and the 96-well dish was covered and incubated at 37°C for 30 min. Fluorescence was measured at 485 nm excitation and 530 nm emission wavelengths using a FlexStation 3

Microplate Reader (Molecular Devices, San Jose, CA, USA). Relative fluorescence values after gene silencing or FCF treatment were expressed as a percentage of the values obtained on 100% control/non-treated cells.

4.3 Determination of the fusion index

The progress of myotube differentiation was quantified by immunocytochemistry. Cells were seeded on glass coverslips, samples were fixed with 4% paraformaldehyde solution (PFA) at each day of the differentiation process, and subsequently subjected to desmin-specific immunolabelling and DAPI (4',6-diamidino-2-phenylindole) staining (see Immunocytochemistry for a detailed protocol). Confocal images were taken of the corresponding samples. Alexa Fluor 488 and DAPI-labelled samples were imaged using an AiryScan 880 laser scanning confocal microscope (Zeiss, Oberkochen, Germany) with 20x air and 40x oil-immersion objectives. The fusion index was calculated as the ratio of the number of nuclei within myotubes with two or more nuclei to the total number of nuclei in the fields of view.

4.4 RNA isolation and RT-PCR analysis

Samples of cell cultures were collected in Trizol (Molecular Research Center, Cincinnati, OH) reagent and subjected to a general RNA isolation protocol. After adding 20% chloroform, samples were centrifuged at 4°C at 16 000 × g for 15 min. The upper aqueous phase of the samples was precipitated with 500 µl RNase-free isopropanol at room temperature for 10 min. After centrifugation (12 000 × g), the precipitated RNA was washed with 75 V/V% ethanol and centrifuged again. Total RNA was dissolved in RNase-free water, the concentration and purity were determined using a NanoDrop 1000 Spectrophotometer (Thermo Fisher Scientific, Waltham, Massachusetts, USA). After successful isolation, the nuclease-free water samples were stored at -80°C. Reverse transcriptase (RT) reaction mixture (20 µl) (Omniscript, QIAGEN, Germantown, MD, USA) contained 1 µg RNA, 0.25 µl RNase inhibitor, 0.25 µl oligo (dT), 2 µl dNTP (200 µM) in RT buffer. Amplification of chosen cDNA sequences was performed using specific primer pairs designed using Primer Premier 5.0 software (Premier Biosoft, Palo Alto, CA) based on mouse nucleotide sequences published in GenBank and purchased from Bio Basic (Toronto, Canada). The specificity of custom designed primer pairs was verified *in silico* using the NCBI Primer-BLAST service (<http://www.ncbi.nlm.nih.gov/tools/primer-blast/>). Amplifications were carried out in a

programmable PCR instrument (Labnet MultiGene 96-well Gradient Thermal Cycler; Labnet International, Edison, NJ) with the following settings: initial denaturation at 94°C for 1 min, followed by 30 cycles of denaturation at 94°C (30 s); annelation at optimized temperature for each primer pair for 30 s, extension at 72°C for 60 s, ended by final elongation at 72°C for 5 min. The PCR products were mixed with EZ-Vision Dye 6X (VWR) and DNA bands were visualized after electrophoresis on 1.2-2.5% agarose gel (Fujifilm Labs-3000 device, Fuji, Tokyo, Japan).

4.5 Gene knockout using CRISPR/Cas9 method

The CRISPR/Cas9 knockout (KO) and HDR (Homology-directed repair) plasmid constructs specifically targeting the mouse Septin7 gene in 3 different coding regions (exon #3, #4, and #5) were obtained from Santa Cruz Biotechnology (Santa Cruz, Dallas, Texas, USA). The Septin7 CRISPR-Cas9 KO plasmid contained a set of 3 different guideRNA plasmids and HDR plasmids. Sense A: TCAGCAACCGAAGAACCTTG (exon3), Sense B: CTGACAATAGTTGATACTCC (exon4), Sense C: CTGGAGAATACAAATCTGTG (exon5).

C2C12 cells were transfected with KO and HDR plasmids in serum-free Opti-MEM solution (Invitrogen) using Lipofectamine 2000 transfection reagent (Invitrogen). After 48 h, cells were maintained in puromycin-containing selection medium (2 µg/ml) for 5 days, and then the corresponding individual cells were selected based on their GFP (Green Fluorescent Protein) and RFP (Red Fluorescent Protein) protein expression from the vectors, using a FACS Aria flow cytometer (BD Biosciences, San Jose, CA). Cells were placed in proliferating medium and cell division was monitored using a transmission microscope (EVOS XL Core Imaging System, Thermo Fischer Scientific).

4.6 Gene silencing

C2C12 cells were cultured in a 6-well dish. After reaching 50-60% confluence, serum-free Opti-MEM solution was applied to the cells and transfection was performed using Lipofectamine 2000 (Invitrogen) transfection reagent with a retroviral pGFP-V-RS vector containing a Septin7-specific shRNA (short hairpin RNA) construct. Cells were treated with a shRNA vector of mixed sequence (Scr cells) as a control. 3 hours after transfection, cells were allowed to regenerate and synthesize the encoded shRNA for 48 h in a proliferating media. After the incubation period, cells were selected in culture medium containing Puromycin (2 µg/ml) until well-defined cell clones appeared in the culture dish. The individual clones were

placed in separate culture dishes and, once a sufficient number of cells had been obtained, the efficiency of gene silencing was verified at the protein level by Western blot. Clones showing a significant reduction in Septin7 expression were tested after several passages and only those in which reduced Septin7 protein expression was consistently detected (S7-KD cells) were used for subsequent experiments.

4.7 Preparation of a fluorescently labeled fusion protein and transfection of cells

Septin7-N-mCherry and Septin7-N-ECFP (Enhanced cyan fluorescent protein) coding sequences were cloned into pcDNA 3.1(+) expression vector (Thermo Fisher Scientific). After reaching 50-70% confluence, serum-free OptiMEM culture medium was applied to the cells and the vectors encoding the fusion proteins (mCherry or ECFP) were transfected using Lipofectamine 2000 (Invitrogen) reagent. Three hours after transfection, media was exchanged to proliferation medium and further analysis of the samples was performed after 24 or 48 hours. Before live cell microscopy, nuclei were stained with Hoechst 33342. Images were acquired using an AiryScan 880 laser scanning confocal microscope (Zeiss).

4.8 Tracking fluorescently labeled fusion protein expression in living cells

C2C12 cells were grown on 96-well Cell Carrier Ultra plates (6055302, Perkin Elmer, Waltham, MA, USA) in DMEM containing 10 V/V% FBS. At 70% confluence level, the culture medium was exchanged to serum-free Opti-MEM and cells were transfected with plasmid encoding Septin7-N-mCherry. The cells were allowed to express the encoded protein for 24 hours. For cultures with nearly 95-100% confluence, a cell-free zone was created using a Tecan Freedom EVO robot, using the liquid handling arm with a pipette tip of 10 μ l. Images were acquired on an Opera Phenix High Content Confocal System (Perkin Elmer, Waltham, MA, USA). A total of 24 fields with 200-250 cells per well were acquired, and a laser-based autofocus was used for each imaging position. Images of the transverse and Alexa-647 channels were collected at the 5 μ m position of the Z image plane relative to the bottom of the optical disc using a 63 \times objective (NA: 1.15).

4.9 Immunocytochemistry

After washing with PBS, the cells were fixed in 4 V/V% paraformaldehyde (PFA) solution for 15 min. Excess paraformaldehyde was inactivated using PBS containing 0.1M glycine. To permeabilize the cells, PBS solution containing 0.25 V/V% Triton-X (TritonX-100, Sigma) was

used for 10 min followed by three PBS washes (3x15 min). Then, serum-free protein blocking (DAKO, Los Altos, CA, USA) was used for 30 min. After blocking, primary Septin7 antibody (IBL, 1:250) diluted in blocking solution was applied to the samples and incubated for 16-18 h in a humid chamber at 4°C. After the incubation period, the samples were washed with PBS (3 x 15 min) and then the secondary fluorophore-conjugated antibody (1:1000), FITC-phalloidin (1:1000) or TRITC-phalloidin (1:1000) were applied to the samples for 1 h at room temperature. The fluorophore conjugated with phalloidin binds specifically to F-actin. After three washes in PBS (3x 15 min), the preparation of the samples was completed using coverslips. Images of Alexa Fluor 488, TRITC, FITC, Hoechst33342 and DAPI labelled samples were acquired using an AiryScan 880 laser scanning confocal microscope (Zeiss) with 20x air and 40x and 63x oil immersion objectives. For excitation of the secondary antibodies and/or fusion proteins (Septin7-N-mCherry and Septin7-N-ECFP) wavelengths of 488 nm, 543 nm and 405 nm were used, depending on their fluorescence detectability, while emission at long wavelengths was collected with a long-pass filter above 550 nm.

4.10 Detection of mitochondria in C2C12 cells

C2C12 cells were plated onto glass coverslips and after 24 h, according to the manufacturer's protocol, mitochondria were labeled with MitoTracker™ Red CMXRos (Thermo Fisher Scientific) stain and fixed according to the immunocytochemistry protocol for further analysis.

4.11 Colocalization study

Colocalization of actin and Septin7 filaments was performed after immunolabelling using an AiryScan 880 laser scanning confocal microscope (Zeiss) and Zeiss 3.5 Blue software. The results of the fluorescence colocalization studies were also plotted graphically in scatter plots, where the intensity of one color was plotted against the intensity of the second color for each pixel. In the scatter plots, Pearson's correlation coefficient (PCC) was used to quantify colocalization. The PCC formula is given below for a typical image consisting of red and green channels:

$$\text{PCC} = \frac{\sum_i (R_i - \bar{R}) \times (G_i - \bar{G})}{\sqrt{\sum_i (R_i - \bar{R})^2 \times \sum_i (G_i - \bar{G})^2}}$$

where R_i and G_i refer to the intensity values of the red and green channels, respectively, and the intensity value of pixel i , and \bar{R} and \bar{G} refer to the average intensity of the red and green channels

in the whole image. The PCC values range from 1 for two images with perfectly linearly related fluorescence intensities to -1 for two images with perfectly but inversely related fluorescence intensities. Values close to zero reflect the distribution of samples that are not correlated.

4.12 Determination of Septin7 filament thickness

Quantification of changes in the structure of the Septin7 filament was evaluated by determining the thickness of Septin7 filaments in fluorescence images of control (Ctrl) C2C12 cultures. After 24 h FCF treatment (100 μ M, Sigma) C2C12 cells were labelled using the method described in the Immunocytochemistry section and images of the samples were acquired using an AiryScan 880 laser scanning confocal microscope. The images were processed using Zen 3.5 Blue software, where five regions were randomly selected within each cell and their thickness was determined from the fluorescence intensity of the labeled Septin7 filaments.

4.13 Protein detection (Western Blot)

Cells were collected in lysis buffer (20 mM Tris-HCl, 5 mM EGTA, Protease Inhibitor Cocktail [Sigma, St. Louis, USA]). Protein concentrations of the samples were determined using BCA protein assay, 5x electrophoresis sample buffer (20 mM Tris-HCl, pH 7.4, 0.01% bromophenol blue dissolved in 10% SDS, 100 mM β -mercaptoethanol) was added to the total cell lysate and boiled at 95°C for 5 min to denature the proteins. Using 7.5% SDS-polyacrylamide gel, 8-10 μ g of total protein sample (Septin7) was electrophoretically separated. The proteins were then transferred onto nitrocellulose membrane and blocked with 5% non-fat milk dissolved in PBS. The membranes were incubated with the corresponding primary antibodies (Septin7, IBL, 1:250, α -actinin, Sigma, 1:250) for 16-18 hours at 4°C. After binding, a 30 min PBS+1V/V% Tween-20 (PBST) wash was followed by incubation with HRP-conjugated secondary antibodies at room temperature. Detection of specific binding was performed by amplified chemiluminescence (Thermo Fisher Scientific). Densitometry analysis of the signals was performed using ImageJ software (NIH, Bethesda, MD, USA). Semiquantitative comparison of signals was performed using ImageJ software, and the detected Septin7 signal was normalized to the alpha-actinin signal of the same sample. To compare the Septin7 signals detected in Scr and S7-KD samples, the values were normalized to the Septin7 value obtained in Ctrl cells, so that the values were also expressed as %. Assays were performed on at least three independent samples and the number of technical replicates was also set to three.

4.14 Investigating cell migration

Cells (2×10^4) were plated in a special insert (Ibidi GmbH, Gräfelfing, Germany) and allowed to adhere to the surface for 24 hours. Before removing the insert, Mitomycin C (Sigma) treatment (10 $\mu\text{g}/\mu\text{L}$, 2 h) was applied to block cell division. After incubation, the media containing Mitomycin C was exchanged, the cells were washed with PBS, and after removal of the insert, proliferation media containing solvent control (ethanol, Sigma) or FCF (100 μM , Sigma) was added to the cells. Cell migration was monitored in a CytoSMART™ system (CytoSMART Technologies, Eindhoven, The Netherlands; Lonza Bioscience, Basel, Switzerland) at 37°C in a 5% CO₂ thermostated environment. The system captured images from the settled field of view every 5 min, at the end of the experiment a 24-h video was available. The system used a 20× objective. The images captured by the CytoSMART™ system were individually saved from the videos and analyzed further using ImageJ software (National Institutes of Health, Bethesda, MD, USA, <https://imagej.nih.gov/ij/>). To analyze the migration of individual cells, we used the MathLab (MathWorks) based Cell Tracker image processing software. We calculated the total distance travelled, the maximum distance reached from the starting point, the average velocity, and also displayed the migration paths of each analyzed cell. During the 12-hour measurement, we calculated the number of times the cells did not move. The movement of each cell in any direction was determined in 20-minute time windows of the original recordings. Cells were considered to be moving if their displacement in any direction exceeded the diameter of the cell, otherwise they were considered to be non-moving for the time period.

4.15 Measuring intracellular $[\text{Ca}^{2+}]$

Cells were loaded with Fura-2-AM (Sigma) calcium indicator for 20 min at 37°C in serum-free culture medium (DMEM, 2.5 μM Fura-2-AM). After loading, cells were maintained in Tyrode's solution (in mM: 137 NaCl, 5.4 KCl, 0.5 MgCl₂, 1.8 CaCl₂, 11.8 Hepes and 1 g L⁻¹ glucose; pH 7.4). Fura-2 was excited with a CoolLED pE-340fura light source (CoolLED LTD, Andover, England) coupled to a ZEISS Axiovert 200m inverted microscope (Zeiss). The excitation wavelength varied between 340 and 380 nm, the emission was detected with a band-pass filter at 505-570 nm, the measurements were performed at room temperature. Image acquisition and post-processing were performed using AxioVision (rel. 4.8) software (Zeiss). The fluorescence coefficient representing $[\text{Ca}^{2+}]_i$ was calculated from images taken at 340 and 380 nm after

background correction. Two objectives were used in these experiments, 10× (air) for data acquisition and 40× (oil immersion) for representative images.

4.16 Statistical and data analysis

The pooled data are expressed as mean \pm standard error of the mean (SEM). Differences between data groups were evaluated using ordinary one-way ANOVA, Bonferroni post hoc multiple comparison test (GraphPad Software, San Diego, CA, USA) and Student's t-test (two sample), where p-values less than 0.05 were considered statistically significantly different.

5 Results

5.1 Expression of different septins in C2C12 myoblasts and differentiated myotubes

In C2C12 cells, mRNAs of different septin proteins were detected during proliferation and differentiation. At mRNA levels of the representatives of SEPT2 group (1,2,4,5), *Septin1* was barely expressed, *Septin2* was detected in both proliferating and differentiating samples, *Septin4* showed differentiation-dependent expression, and *Septin5* was also present. From the SEPT3 (3,9,12) group, *Septin3* was barely expressed and *Septin12* was not detectable, whereas *Septin9* showed nice signals in both proliferating and differentiating samples. From the SEPT6 group members (6,8,10,11,14), *Septin14* was not amplified in the samples we tested, while mRNAs of the other proteins were detected in both proliferating and differentiating samples. Of particular importance is the presence of *Septin7*, the only member of the SEPT7 group, as this protein is required for the formation of septin complexes. *Septin7* mRNA was detectable in both proliferating and differentiating samples. Since septins form different types of macromolecular complexes and hetero-oligomers with each other, the presence of a specific group of septin proteins is critical for the organization of the corresponding protein complex. For detailed information, we also examined the expression of *Septin7* at the protein level in C2C12 cultures at different developmental stages. Our results showed the presence of *Septin7* protein in both proliferating cells and at different days of differentiation. According to semi-quantitative results of normalizing *Septin7* level to the expression level of α -actinin, its expression decreases with the progression of differentiation in C2C12 myotubes.

5.2 Septin7 is essential for C2C12 cell division

To describe the role of Septin7, first we wanted to modify genetically the expression of the protein. Using CRISPR/Cas9 technique to inhibit the expression of Septin7 in C2C12 cells, the experimental approach led to abnormal cell size, in addition, cell division was arrested. These effects were illustrated by the large size of the cells containing multiple nuclei, and cells were not separated from each other. These findings suggest that the presence of Septin7 is essential for the appropriate division of C2C12 cells, on the other hand, the use of a different gene modification method was required to generate a sustainable Septin7-modified cell line for further experiments.

5.3 Effects of reducing Septin7 protein expression in C2C12 cells

Altered expression of Septin7 in C2C12 myoblasts was achieved by shRNA-mediated gene silencing. Reduced protein levels of Septin7 were detected in knockdown (S7-KD) cells as compared to absolute control (Ctrl) and cells transfected with mixed Septin7 shRNA sequence (Scr). Approximately 50% reduction in Septin7 protein expression was achieved by gene silencing and the reduction of Septin7 expression was maintained during differentiation.

Monitoring the gene-silenced cells under transmitted microscope, we observed that reduced the expression of the Septin7 protein resulted in significant changes in both cell morphology. To detail these changes, specific immunolabelling for Septin7 and actin (F-actin, which fundamentally affects cell shape) was performed on Scr and S7-KD cells. The characteristic Septin7 filament structure observed in Ctrl and Scr cells disappeared in most S7-KD cells, and instead a fragmented, pointwise appearance of the protein was observed. In Ctrl and Scr cultures, the Septin7 and actin filaments were highly co-localized, whereas in S7-KD cells this spatial overlap was not present, although the intracellular actin structure appeared mostly unchanged. A colocalization study was also performed for Scr and S7-KD cultures, showing that the Pearson's coefficient was lower in S7-KD cells (0.648) than in Scr C2C12 cells (0.833). To quantitatively characterize the changes in cell morphology, the ImageJ program was used to determine the area (T), perimeter (K) and the circularity (C) of individual cells in the above-mentioned cell cultures. Circularity is a dimensionless number between 0 and 1, calculated by the formula $(4\pi \times T / K^2)$. The mean area and circularity of S7-KD cells were significantly higher compared to the corresponding parameter of Scr cultures (S7-KD: T= 1564±142 μm^2 ; p<0.05; n=121, C=0.58±0.05; p<0.001, Scr: T= 1348±138 μm^2 and C=0.47±0.05; n=96). This result correlates well with our previous observations that S7-KD cells had less projections. We also

determined the perimeter of each cell type and found no difference between Ctrl ($190.1 \pm 16.9 \mu\text{m}$), Scr ($196.5 \pm 19.9 \mu\text{m}$) and S7-KD cultures ($185.0 \pm 16.7 \mu\text{m}$). No significant differences were found between Ctrl and Scr cells in all parameters we calculated (Ctrl: $T=1298 \pm 115 \mu\text{m}^2$ and $C=0.46 \pm 0.04$; $n=127$), suggesting that reduced Septin7 expression has a significant role in the differences revealed in S7-KD cells' morphology. The decrease in Septin7 expression could also adversely affect higher order structures of the septins.

We tested the proliferative capacity of myoblasts over several days and found significantly reduced cell division in Septin7 modified cells (data normalized to Ctrl cells, Scr: $94.1 \pm 7\%$, S7-KD: $79.7 \pm 5.2\%$, $N=3$, $n=24$; $p < 0.001$). This correlates well with the observation, that S7-KD cells reached confluence later than Scr or Ctrl cultures even starting with the same cell number.

5.4 Septin7 is essential for the differentiation of C2C12 cells

Another observation was that the formation of myotubes during the differentiation of the cultures was also significantly altered following the gene silencing of Septin7. To determine this finding precisely, the cultures were fixed on different days of differentiation and immunolabeled for desmin. Desmin was only observed after the fusion of the myoblasts into multinucleated myotubes. From the second day of differentiation, increasing myotube formation was observed in Ctrl and Scr cultures, while only negligible cell fusion was detected in S7-KD cultures, even on day 6. To characterize the changes quantitatively, we determined the fusion index in each culture on the given differentiation days. For the Ctrl and Scr cultures, we obtained steadily increasing values, representing a progressively more advanced degree of differentiation (higher number of nuclei within the myotubes). In contrast, in the S7-KD cultures, we obtained significantly lower fusion indices from the second day of differentiation, indicating a retarded state of myotube formation ($N=2$, $n=20$ per cell type and values in %, Ctrl: D2: 23.2 ± 2.5 ; D3: 34.6 ± 4.1 ; D4: 38.7 ± 3.1 ; D5: 49.9 ± 3.5 ; D6: 60.9 ± 2.95 ; Scr: D2: 25.3 ± 3.8 ; D3: 32.5 ± 3.2 ; D4: 38.9 ± 3.7 ; D5: 44.1 ± 3.5 ; D6: 53.8 ± 2.9 ; S7-KD D2: 3.8 ± 1.3 ; D3: 8.6 ± 2.0 ; D4: 10.7 ± 1.2 ; D5: 10.4 ± 2.4 ; D6: 12.6 ± 1.8 ; $p < 0.05$).

5.5 Effect of Septin7 on the mitochondrial network of C2C12 cells

After staining live cells with MitoTracker Red CMXR, we found that not only the filamentous structure of Septin7 was different in S7-KD cells, but also the mitochondrial network was

severely affected. The extensive mitochondrial "network" observed in Ctrl and Scr cultures showed a significantly narrowed and modified complexity in S7-KD cells. This may suggest that the cytoskeletal septin system may also play an important role in the assembly and maintenance of mitochondrial structure in myoblasts.

5.6 Septin7 has a different arrangement in migrating and non-migrating cells

We have demonstrated that Septin7 and actin filaments, the latter of which is well known to play a regulatory role in cell motility, co-localize in C2C12 cells. However, no information was available on the structural rearrangement of the Septin7 protein during myoblast migration. In non-migrating cells, we detected a filament-like appearance of Septin7, but during migration this expression pattern changed and well-organized structural units were formed, mainly observed in cell projections and trailing edges. As an approximate 50% reduction in protein expression was achieved, S7-KD cells are essentially able to produce Septin7, and the appearance of filaments was also detected in cell protrusions in migrating S7-KD cells. During migration, the altered appearance of Septin7 is accompanied by a reorganization of the actin system in all cell types examined.

We monitored the appearance of the Septin7 protein over time by expressing fluorescently tagged Septin7-N-mCherry protein from exogenous plasmids using the Opera Phenix imaging system. The newly formed Septin7 showed a filamentous appearance under normal culture conditions, and using immunolabeling we could distinguish fluorescent filaments expressed from the plasmid from those formed endogenously. In addition, the expression of the fusion protein was monitored in migrating C2C12 myoblasts. Based on 5 min recordings, a continuously changing pattern of Septin7 filaments was observed, providing clear evidence for changes in Septin7 filaments during migration.

5.7 Septin7 plays a role in intracellular $[Ca^{2+}]_i$ changes during migration

Non-migrating (NM) and migrating (M) cells can clearly separate in cell cultures kept in serum-free DMEM medium after 5 h incubation. Since C2C12 myoblasts are unable to divide under the aforementioned condition, the change in $[Ca^{2+}]_i$ was associated with cell migration. There was no significant difference in $[Ca^{2+}]_i$ between non-migrating Ctrl and Scr cells (F_{340}/F_{380} ratio values, Ctrl: 2.64 ± 0.07 ($n_{NM} = 48$), and Scr: 2.52 ± 0.05 ($n_{NM} = 62$)), while migrating cells from

these cultures showed a significant increase in $[Ca^{2+}]_i$ as compared to their non-migrating counterparts (F_{340}/F_{380} ratio values, Ctrl: 3.02 ± 0.03 ($n_M=89$), and Scr: 3.20 ± 0.05 ($n_M=86$); $p < 0.001$, both cases). In non-migrating S7-KD cells lower, but significantly not different $[Ca^{2+}]_i$ level was measured as compared to Scr cells (F_{340}/F_{380} ratio values, S7-KD: 2.39 ± 0.04 ($n_{NM}=130$)). Although elevation in the $[Ca^{2+}]_i$ was observed in migrating S7-KD cells (S7-KD: 2.79 ± 0.04 ($n_M=125$), $p < 0.001$) similar to Ctrl and Scr myoblasts, this elevation was much smaller in proportion.

5.8 The level of Septin7 affects migration

Since the arrangement of Septin7 filaments differ in migrating and non-migrating cells, we wanted to determine the basic parameters of migration (total distance travelled, average speed, maximum distance from the origin) in Septin7 gene silenced C2C12 cell line. Measurements were performed for 24 h, of which the first 12 h were used for data analysis (3 independent experiments per cell line). Our results show that the average velocity of S7-KD ($n=33$) cells (0.71 ± 0.02 $\mu\text{m}/\text{min}$) was higher than that of Scr ($n=34$) cells (0.58 ± 0.02 $\mu\text{m}/\text{min}$, $p < 0.001$), and these cells moved further away from the origin (S7-KD: 311.64 ± 15.43 μm , Scr: 251.57 ± 10.16 μm ; $p < 0.01$). The total distance travelled was also longer for S7-KD cells than for Scr cells (S7-KD: 509.32 ± 15.18 μm and Scr: 416.18 ± 12.76 μm ; ($p < 0.001$). The difference between Scr and S7-KD cells is also illustrated by the number of non-migrating events, which was significantly higher in Scr cells.

It is important to highlight that no significant changes were observed between Ctrl ($n=23$) and Scr cells in the parameters studied during 12 h of migration (velocity: 0.54 ± 0.02 $\mu\text{m}/\text{min}$, total distance travelled: 383.43 ± 13.93 μm and maximum distance from origin: 329.54 ± 19.9 μm), suggesting that migration pattern change is due to reduced expression of the Septin7 protein.

5.9 FCF stabilizes Septin7 filaments in C2C12 myoblasts

We further investigated whether FCF treatment affects the proliferation of C2C12 myoblasts. After 24 hours of FCF treatment, we evaluated the changes in cell division using CyQuant assay and found that the drug dose-dependently reduced cell proliferation ($IC_{50}=180.8$ μM , $R^2=0.8671$). For further studies, we chose a concentration of 100 μM . Following FCF treatment of myoblasts, Septin7-specific immunolabeling was performed to monitor changes in filament structure. We found that the architecture of Septin7 filaments was significantly altered by FCF, with longer and thicker filaments appearing in cells, in addition, their intracellular location was

different as compared to the untreated cells. The thickness of filaments was also quantified within the corresponding Ctrl cells (5 randomly selected areas per cell for 4 individual cells in both cases). Based on our results the thickness of immunolabeled Septin7 filaments was significantly greater in FCF-treated cells compared to their corresponding units in untreated cells (670.5 ± 20.1 nm; $n_{\text{filament}}=57$ in untreated and 973.3 ± 34.3 nm; $n_{\text{filament}}=63$ in FCF-treated Ctrl cells; $p < 0.001$). Subsequently, the aforementioned FCF treatment and immunolabeling were repeated on cells transfected with the fusion protein, and the appearance of larger size fluorescently tagged filaments was observed on treated cells, similar to endogenous Septin7.

5.10 FCF treatment altered migration of C2C12 myoblasts, but C2C12 S7-KD cultures were more resistant to the treatment

The FCF treatment affected the parameters of migration in all cell cultures, but the changes of the parameters were different. The parameters of Scr ($n=37$) and Ctrl ($n=21$) cells were significantly reduced by the treatment (Scr and Ctrl treated and untreated, $p < 0.001$) compared to their untreated counterparts (Scr FCF treated: velocity: 0.35 ± 0.02 $\mu\text{m}/\text{min}$, total distance travelled: 249.15 ± 13.08 μm and maximum distance from origin: 139.03 ± 8.21 μm , Ctrl FCF treated: velocity: 0.39 ± 0.02 $\mu\text{m}/\text{min}$, total distance travelled: 279.30 ± 11.09 μm and maximum distance from origin: 183.07 ± 11.53 μm , data for untreated cells are shown in Chapter 5.8). Comparing the parameters of treated Scr and Ctrl cells, they were not significantly different from each other, while S7-KD ($n=32$) cultures appear to be more resistant to FCF treatment (S7-KD FCF treated: velocity: 0.63 ± 0.02 $\mu\text{m}/\text{min}$, total distance travelled: 452.39 ± 16.57 μm and maximum distance from origin: 227.42 ± 9.35 μm , $p < 0.05$, for non-treated data see Chapter 5.8), the latter observation possibly due to lower expression of the Septin7. Data so far show that FCF stabilizes the septin filaments in a reversible manner after about 3-4 hours. To demonstrate this effect, we also examined total pathway length data over time, showing that FCF was already effective within the first hour of treatment, and that this effect was more significant in Scr cultures than in S7-KD cells. FCF needed more time to develop an inhibitory effect on migration in S7-KD cells, but after a certain time, about 8 hours of treatment, the drug caused a significant change in the parameter tested as compared to untreated cells. Experiments on Ctrl cells showed that they responded to FCF treatment in a similar way to Scr cells.

6 Discussion

6.1 Septin filaments are an integral part of the skeletal muscle cytoskeleton

Septins are essential elements of the cytoskeletal system, and their absence can lead to various pathological changes. They are regulators of spatial compartmentalization in yeast and thus play a key role in cytokinesis. Septins are GTP-binding proteins that form filaments and higher-order structures in the submembrane layer of the plasma membrane in eukaryotic cells and associate with actin and microtubule cytoskeletal networks. The septin complexes coordinate cell division, contribute to the maintenance of cell polarity and to the dynamic remodeling of the cell membrane structure. Although the expression and role of cytoskeletal septins have been studied in a variety of cell/tissue types, information on skeletal muscle and its model systems is lacking in the literature. To the best of our knowledge, our results are the first to describe the ontogenesis-dependent expression of RNA of different septin proteins in C2C12 myoblast cells and during their differentiation in myotubes of different maturity. Members of the four septin groups (SEPT2, SEPT3, SEPT6, SEPT7) are expressed in C2C12 cells, which provide the opportunity to generate diverse septin oligomers and higher-order structures. Based on our experiments, we have demonstrated that the Septin7 protein, as the only member of its group, shows a decreasing expression with progression of differentiation. This suggests that its role is more important during the initial stages of myoblast proliferation and differentiation, when most cell fusion occurs.

6.2 The role of septins in the regulation of cellular biology of myoblasts

The interaction between septins and other cytoskeletal proteins plays a prominent role in the conversion of mechanical signals into biochemical responses. Septins are involved in mechanotransduction by promoting the formation of contractile actomyosin networks. Several attempts have been made to generate gene knockout septin model systems, however, only 7 types of septin knockout mice have been generated from the 13 currently known septin proteins. Genetic ablation of the ubiquitous *Septin7*, *Septin9* and *Septin11* has resulted in embryonic lethality. *Septin7*^{-/-} mice were never born, arrested early in development, probably due to mitotic defects, showing mesenchymal tissue degeneration and extensive cell death.

Consistent with the above, we demonstrated co-localization of Septin7 and actin filaments in Ctrl and Scr C2C12 cells. Our results indicate that without Septin7 these cells are unable to divide, CRISPR-Cas9 gene knockout technology was unsuccessful, resulting in giant cells with

multiple nuclei that unable to proliferate. Using gene silencing, we achieved about 50% reduction of Septin7 protein level in C2C12 cells, which altered the structure, size, and shape of the filaments. Our results are in agreement with the scientific literature, as the process of gastrulation does not occur in Septin7-deficient mouse embryos, suggesting a key role for Septin7 during individual development.

In our experiments, the absence of the Septin7 protein resulted in larger cells with smaller and less elongated, almost round myoblast cells with significantly modified intracellular Septin7 filaments. This correlates with the observation that Septin7 has a crucial function in determining cell morphology in different cell types, such as neurons of dorsal root ganglia of the nervous system or primary fibroblasts of mice. In the model system we studied, a reduced expression of Septin7 protein caused a decrease in the proliferation of C2C12 myoblasts.

In addition, S7-KD myoblasts have a significantly inhibited capability for formation of multinucleated myotube, therefore, their differentiation program is impaired. During differentiation, the expression of several transcription factors at a given time is crucial, but in addition to cellular coupling, rearrangement of the cytoskeletal system is also required for the generation of myotubes. Studies on C2C12 myoblasts have identified RhoA, Rac1 and Cdc42 as important regulators of myogenesis. These GTPases function by modulating the activity of downstream kinases and transcription factors such as p38 MAPK, c-Jun N-terminal kinases (JNK) and serum response factor (SRF). The complex signaling pathways, which are regulated by these proteins in C2C12 cells, in relation to septins have not yet been investigated, so it is currently only speculated that these pathways may influence differentiation via the Septin7 protein.

To summarize our observations, we first described that Septin7 is a key player in the regulation of cytoskeletal septin organization, cell morphology, proliferation, and differentiation in C2C12 myoblasts, parameters that are essential for myogenesis and regeneration. Although a Septin7 KO mouse model does not exist, a skeletal muscle-specific knockdown model was generated by our group, which provided an opportunity to study skeletal muscle processes.

Mitochondria are key organelles that regulate cellular metabolism through an integrated mechanism of energy production via oxidative phosphorylation. The overall morphology of the network is determined by mitochondrial fusion and fission, in which the mitochondrial fission regulator Drp1, which has been linked to the protein Septin2, plays a major role. Our observations suggest that Septin7 may have a role in mitochondrial fusion and fission, but further experiments are needed to prove this hypothesis.

6.3 The rearrangement of Septin7 filaments has a major importance in migrating myoblasts

Some publications have already discussed that modifying the expression of specific septin proteins (in some cases Septin7) alters the migration of different eukaryotic cell types. Alterations have been observed in microvascular endothelial cells, human epithelial cells, human breast cancer cells and lung cancer cells, among others, but skeletal muscle cell migration has not been investigated in this respect.

In the present study, we show that the intracellular architecture of Septin7 is different in non-migrating and migrating myoblasts. In non-migrating cells, Septin7 filaments are present throughout the cytoplasm, whereas in migrating cells a more specific localization of filaments is observed, especially in cell projections and the trailing edge. In migrating S7-KD cells, the appearance of Septin7 filaments was observed, but their length and size were lower than those of Scr cells. The role of Septin7 in migration has been reported, but the exact mechanism of whether cell-specific environmental factors can alter the behavior of the protein is not yet fully understood. It is well known that cell polarization requires the formation of separate rear and front end of the cell, which is important for directed migration and cell movement. The actin-mediated lamellipodial membrane elevation forms the edge of the migrating cell, and the formation of the retractile tail is crucial for the execution of movement. The specific appearance of actin filaments is seen in all our cell types, but their intracellular distribution is altered in S7-KD cells, contributing to a more spherical and less elongated cell morphology. Whereas in Ctrl and Scr cells, Septin7 and actin co-localize and the boundaries are largely visible, in S7-KD cells the random distribution and pointwise appearance of Septin7 filaments is less related to the actin system. The above-mentioned changes in S7-KD cells contribute significantly to the different cell shape and cytoskeletal organization of migrating cells. However, it is important to highlight that reduced Septin7 expression did not inhibit migration of C2C12 cells.

6.4 Altered Septin7 protein expression has a significant effect on myoblast migration

Dynamic adaptation of $[Ca^{2+}]_i$ homeostasis during migration is essential in all cell types. In migrating cells, an increasing anterior-posterior $[Ca^{2+}]_i$ gradient is formed, which plays a role in the resolution of focal adhesions, cell posterior retraction and motility. The anterior-posterior polarity must be maintained during migration because this biochemical process is necessary to block lamellipodia formation at the rear end of the cell. In our measurements, we found that resting $[Ca^{2+}]_i$ did not differ significantly between Ctrl, Scr and S7-KD myoblasts, while $[Ca^{2+}]_i$

increased during migration for all cell types. Our observations show that $[Ca^{2+}]_i$ was significantly lower in migrating S7-KD cells than in Scr and Ctrl cells, which may be related to the reduced Septin7 protein level. Several studies have already addressed the relationship between septins and cytoplasmic $[Ca^{2+}]_i$ regulation. Septin7 has been shown to regulate Ca^{2+} entry via Orai channels in human neural progenitor cells and neurons. In addition, there is a demonstrated link between overexpression of dseptin7 in wild-type *Drosophila* neurons and altered $[Ca^{2+}]_i$ homeostasis, which led to significant flight defects in that model system. Our results suggest that reduction of Septin7 expression may alter $[Ca^{2+}]_i$, which may regulate migration and its parameters in myoblasts. Further studies are needed to elucidate the exact mechanism underlying these changes and the related signaling pathways.

Migration is a key process in which cell movement is controlled by coordinated signaling pathways. The small GTPases of the Rho family, mentioned above, may also regulate migration processes, as has been shown in several studies. Among the Rho GTPases, Cdc42 and its interacting partners are often analyzed together with septins. For example, studies in hematopoietic stem cells have reported that the Cdc42-Borg4-Septin7 axis regulates cell polarity. Recent findings suggest that the expression level of Septin7 can either increase or decrease migration parameters. Overexpression of Septin7 caused inhibition of migration in glioma cells, whereas in breast cancer cell lines this change enhanced migration. In the present work, we show that under reduced expression of Septin7, S7-KD myoblasts migrated faster and over greater distances than cells from Scr cultures. To resolve the controversy about the effects of changes in Septin7 expression on cell motility, the limitations of the different experimental setups used to analyze cell migration must be considered. Migration experiments involve the creation of some kind of gap (cell free zone), either by scratching or by using an insert. A 24-hour time limit should be observed during assays, as beyond this it is difficult to determine whether the gap is closed due to cell proliferation and/or migration. In our present experiments, we used a culture inoculum to keep the cells bordering the gap intact. Cells were also treated with Mitomycin C to block cell proliferation. In addition, in our experiments, myoblasts were allowed to migrate in all directions and no specific chemotaxis was applied. Different cell types can migrate either alone (myoblasts), in loosely associated populations (mesenchymal cells), or together as a single cell layer (*e.g.* epithelial cells). Although S7-KD cells migrated faster and over greater distances compared to Scr cells, the formation of myotubes was significantly inhibited in this cell population. By comparing our results with available literature data, we conclude that Septin7 plays a role in the migration of myoblasts, indicating the importance of this protein in myogenesis and muscle regeneration. However, it should also be mentioned that

in vivo, myoblasts have to migrate across the basement membrane and connective tissue barriers, such as the perimysium or endomysium. Furthermore, these processes also require the role of several other regulatory proteins not investigated in this thesis, as the efficient repair and regeneration of skeletal muscle also needs a coordinated remodeling of the extracellular matrix (ECM). To give an example, matrix metalloproteinases (MMPs) play a key role in ECM remodeling during muscle regeneration. In summary, our results suggest that during skeletal muscle development and regeneration, the protein Septin7 may play an important regulatory role.

6.5 Pharmacological inhibition of the dynamic rearrangement of the septin system significantly affects the migration of myoblasts

The ability of septins to assemble into hetero-oligomeric complexes and form higher-order structures is critical for the function of many cells. Septins can be converted *in vitro* into non-polar polymers from recombinant or purified proteins. However, we do not yet know whether these linear filaments reflect how septins are organized into the larger super-structures observed *in vivo*. There are also many questions about the organization of septins in cells, for example, do all higher-order septin-based structures share a common organization at the molecular level? Also, how fast does the transformation of larger septin units (*e.g.* ring, gauze-like form) occur? Based on the literature data, a precise description of the molecular mechanisms underlying the function of heteromeric and higher order septin complexes is currently incomplete. Some research has also suggested that any given septin protein from the same structural group may be a substitute for each other in the complex. This suggests that there could be 20 viable hexamers and 60 octamers, but the generality of this theory is not yet fully proven and has been based on *in silico* modelling. Consequently, there is growing evidence that the literature on septins and structural predictions should be critically evaluated. The analysis of the Septin2 and Septin7 complexes suggests that they function as a kind of base or core within the protein complex. Since the remodeling of higher order septin complexes is quite dynamic and they play a role in many cellular processes, any possibility that may influence this process may be a focus of septin research.

FCF is a plant cytokinin and can reversibly stop the dynamic rearrangement of septins. Our data are in agreement with results from other studies showing that FCF treatment negatively affected cell division, reduced the total distance travelled and the average velocity during migration in C2C12 myoblasts. However, some off-target effects have been published for FCF and septins, which calls into question the specificity of the agent. In our experiments, the efficacy of

mCherry to stabilize Septin7 appears to be specific, since mCherry-tagged Septin7 responded in a similar manner to endogenous for the application of the agent, forming large filaments. The FCF treatment did not alter the migration of S7-KD cells to the same extent as Scr cells, suggesting that these cells are more resistant to the treatment, as the Septin7 protein was not present in such abundance. FCF and its analogues have been mentioned in several lines of research as a potential tumour therapeutic agent. The concentration we used (100 μ M) is of course high and not acceptable as a single agent, however, FCF analogues inhibited the proliferation of certain tumour cell types in the 4-5 μ M range. The target is of course the nM concentration range, thus reducing the potential side effects. At the same time, our measurements could provide an important basis for mapping the side effect profiles of FCF-based agents, for example negative effects on skeletal muscle.

7 Summary

Based on our results, we can state that septin proteins appear differently in the developmental stages of C2C12 cultures. We proved that cells cannot divide without Septin7 and that Septin7 is essential for the formation of myotubes. We have shown that the level of Septin7 contributes to the determination of cell shape, and is an integral part of the cytoskeleton. Our measurements suggest that the level of Septin7 also affects the mitochondrial system of cells, presumably by altering the mitochondrial fusion and fission.

We provide evidence that Septin7 filaments rearrange during myoblast migration. Down-regulation of Septin7 expression resulted in altered parameters of migration, with S7-KD myoblasts moving faster and longer as compared to unmodified cultures. These results may be explained not only by a reduction in the number and structural ordering of septin filaments, but also by the lower alteration of $[Ca^{2+}]_i$ in migrating S7-KD myoblasts. In addition, it appears that S7-KD cells change direction less often as compared to Scr cells, thus "marking" a specific route in which the cell is heading toward. The specific role of Septin7 in the migration of myoblasts is also confirmed by FCF treatment. FCF inhibits C2C12 cell proliferation in a dose-dependent manner and FCF treatment presumably inhibits the dynamic rearrangement of septin filaments. Thus, in our experiments, we observed a marked decrease in parameters of migration in Scr cultures, whereas in S7-KD cultures these changes were almost negligible over the time period we analyzed. Taken together, the Septin7 protein plays a fundamental role in the entirety of myoblast proliferation, differentiation, and migration processes, which are key events in the development and regeneration of functional skeletal muscle fibers.



Registry number: DEENK/424/2023.PL
Subject: PhD Publication List

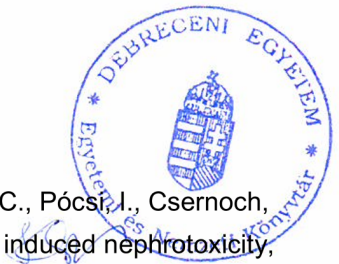
Candidate: Zsolt Ráduly
Doctoral School: Doctoral School of Molecular Medicine
MTMT ID: 10071483

List of publications related to the dissertation

1. **Ráduly, Z.**, Szabó, L., Dienes, B., Szentesi, P., Bana, Á. V., Hajdú, T., Kókai, E., Hegedűs, C., Csernoch, L., Gönczi, M.: Migration of Myogenic Cells Is Highly Influenced by Cytoskeletal Septin7.
Cells. 12 (14), 1825, 2023.
DOI: <http://dx.doi.org/10.3390/cells12141825>
IF: 6 (2022)
2. Gönczi, M., **Ráduly, Z.**, Szabó, L., Fodor, J., Telek, A., Dobrosi, N., Balogh, N., Szentesi, P., Kis, G., Antal, M., Trencsényi, G., Dienes, B., Csernoch, L.: Septin7 is indispensable for proper skeletal muscle architecture and function.
eLife. 11, e75863, 2022.
DOI: <http://dx.doi.org/10.7554/eLife.75863>
IF: 7.7

List of other publications

3. Gönczi, M., Teixeira, J. M. C., Barrera-Vilarmau, S., Mediani, L., Antoniani, F., Nagy, T. M., Fehér, K., **Ráduly, Z.**, Ambrus, V. A., Tózsér, J., Barta, E., Kövér, K. E., Csernoch, L., Carra, S., Fuxreiter, M.: Alternatively spliced exon regulates context-dependent MEF2D higher-order assembly during myogenesis.
Nat Comms. 14, 1329, 2023.
DOI: <http://dx.doi.org/10.1038/s41467-023-37017-7>
IF: 16.6 (2022)
4. **Ráduly, Z.**, Szabó, A., Mézes, M., Balatoni, I., Price, R. G., Dockrell, M. E. C., Pócsfi, I., Csernoch, L.: New perspectives in application of kidney biomarkers in mycotoxin induced nephrotoxicity, with a particular focus on domestic pigs.
Front. Microbiol. 14, 1085818, 2023.
DOI: <http://dx.doi.org/10.3389/fmicb.2023.1085818>
IF: 5.2 (2022)





5. **Ráduly, Z.**, Price, R. G., Dockrell, M. E. C., Csernoch, L., Pócsi, I.: Urinary Biomarkers of Mycotoxin Induced Nephrotoxicity: Current Status and Expected Future Trends.
Toxins. 13 (12), 848, 2021.
DOI: <https://doi.org/10.3390/toxins13120848>
IF: 5.075
6. **Ráduly, Z.**, Szabó, L., Madar, A., Pócsi, I., Csernoch, L.: Toxicological and Medical Aspects of Aspergillus-Derived Mycotoxins Entering the Feed and Food Chain.
Front. Microbiol. 10, 2908, 2020.
DOI: <http://dx.doi.org/10.3389/fmicb.2019.02908>
IF: 5.64
7. Sharma, R., **Ráduly, Z.**, Miskei, M., Fuxreiter, M.: Fuzzy complexes: specific binding without complete folding.
FEBS Lett. 589 (19), 2533-2542, 2015.
IF: 3.519

Total IF of journals (all publications): 49,734

Total IF of journals (publications related to the dissertation): 13,7

The Candidate's publication data submitted to the iDEa Tudóstér have been validated by DEENK on the basis of the Journal Citation Report (Impact Factor) database.

14 September, 2023

